

MALAYSIAN JOURNAL OF ANALYTICAL SCIENCES

Journal homepage: https://mjas.analis.com.my/



Research Article

Synthesis and characterization of magnetized Fe₃O₄-ZrO₂ catalysts for methyl ester production from waste cooking oil

Muhammad Fareez Naufal Fadilah^{1,2}, Balqis Adlina Omar^{1,2}, Farah Wahida Harun², Salina Mat Radzi², and Nurul Jannah Abd Rahman^{1*}

¹Pusat Tamhidi, Universiti Sains Islam Malaysia, Bandar Baru Nilai, 71800 Nilai, Negeri Sembilan, Malaysia ²Faculty of Science and Technology, Universiti Sains Islam Malaysia, Bandar Baru Nilai, 71800 Nilai, Negeri Sembilan, Malaysia

*Corresponding author: jannahrahman@usim.edu.my

Received: 28 August 2024; Revised: 4 December 2024; Accepted: 6 January 2025; Published: 24 April 2025

Abstract

Biodiesel is an efficient, clean, and renewable alternative to petroleum-based fuels. Biodiesel production typically requires heterogeneous catalysts. However, the usage of traditional heterogeneous catalysts faces challenges like difficult recovery and catalyst loss. To address these challenges, this study aims to synthesize and characterize magnetized Fe₃O₄-ZrO₂ catalysts for direct transesterification of waste cooking oil into biodiesel. Fe₃O₄ was first synthesized via co-precipitation of FeSO₄·7H₂O and FeCl₃·6H₂O, resulting in black precipitate. ZrO₂ was then impregnated with 10-30 wt.% Fe₃O₄ using the incipient wetness impregnation method. The catalysts were characterized by thermogravimetric analysis (TGA), Fourier transform infrared spectroscopy (FT-IR), field emission scanning electron microscopy (FESEM), and Brunauer-Emmett-Teller analysis (BET) to assess thermal stability, functional groups, morphology, surface area, and porosity. The catalysts were tested for methyl ester production using 12:1 methanol to waste cooking oil ratio and 5 wt.% catalyst loading at 60°C for 5 hours. The 20Fe-Zr catalyst showed superior performance (13.13%) compared to 10Fe-Zr and 30Fe-Zr catalysts. The enhanced catalytic activity of the 20Fe-Zr catalyst is attributed to its mesopore connectivity, high pore volume, and large surface area. Additionally, its magnetic properties enable easy catalyst separation and demonstrate potential for reuse, making the process more cost-effective and environmentally friendly.

Keywords: methyl ester, magnetize heterogeneous catalyst, waste cooking oil, transesterification

Introduction

Methyl ester, commonly known as biodiesel, is a renewable fuel derived from natural sources such as vegetable oils, animal fats, and recycled cooking oils. It offered a clean alternative to petroleum-based fuels and has garnered significant attention due to its environmental benefits. On August 10, 1893, Rudolph Diesel famously demonstrated the use of vegetable oil to power a diesel engine, illustrating the early potential of biodiesel [1]. As global concerns over climate change, energy security, and the depletion of fossil fuels intensify, biodiesel has emerged as a promising solution. It can be seamlessly integrated into existing diesel engines with minimal modifications, making it the key player in the transition towards a cleaner and more sustainable energy source. However, several properties of vegetable oils, such as their tendency to form gums, high density, elevated free fatty acid (FFA) content, high viscosity, and low volatility, make their direct use in diesel engines impractical and unsuitable [2, 3].

In recent years, the use of vegetable oils as a renewable energy source has gained traction, particularly due to their potential to reduce greenhouse gas emissions [4]. Several methods are employed in biodiesel production, including micro-emulsion, thermal cracking or pyrolysis, transesterification, and direct use of oils or their blends. Among these, transesterification is the most widely used and preferred method due to the high purity of methyl esters produced, making it chemically identical to petroleum diesel [5]. Transesterification efficiently converts lipids and

fats (triglycerides) into alkyl esters with viscosities similar to diesel, enabling biodiesel to be used without modification in conventional diesel engines [5].

Waste cooking oil (WCO) has emerged as an affordable and non-food feedstock for biodiesel Its utilization provides environmentally friendly solution to reduce pollution associated with improper waste disposal. The global rise in human consumption and industrialization of food production has led to an increase in WCO generation, which, if left untreated, can pose significant environmental threats particularly to aquatic ecosystems and wildlife [6, 7]. Therefore, converting WCO into biodiesel not only helps mitigate these environmental concerns but also provides a sustainable alternative to fossil fuels.

In the transesterification reaction, one mole of triglyceride reacts with three moles of alcohol to produce three moles of methyl esters and one mole of glycerol. The process can be reversible [8], and an excess of alcohol is often required to improve ester yields and facilitate phase separation from the glycerol byproduct. The presence of a catalyst, typically a strong acid or base, significantly accelerates the reaction and helps in achieving equilibrium more efficiently. However, there is an increasing demand for cost-effective and sustainable catalysts to make biodiesel production commercially viable [9].

Sodium hydroxide (NaOH) and potassium hydroxide (KOH) are widely used homogeneous catalysts in the production of biodiesel due to their high efficiency and costeffectiveness [10]. However, the use of NaOH and KOH does have some drawbacks, including corrosiveness, hygroscopic nature, potential to cause saponification, and difficulty in separating them from the final product [11]. To address these issues, heterogeneous catalysts have been developed. These catalysts offer several benefits, such as high activity, milder reaction conditions, extended lifespan, ease of separation, reusability, and cost-effectiveness [10]. Another challenge associated with using homogeneous catalysts is the recovery of the catalyst after transesterification, which is crucial for its potential reuse. Efficient recovery of the catalyst is important from both economic and environmental perspectives.

The aim of this study is to explore the potential of Fe₃O₄-ZrO₂ as a magnetized catalyst for direct transesterification of WCO to biodiesel. In this study, magnetized Fe₃O₄-ZrO₂ catalysts were synthesized and characterized using various

analytical techniques. This is a preliminary study to assess the catalytic activity and feasibility of magnetized Fe₃O₄-ZrO₂ in biodiesel production, with a focus on its advantages in terms of ease of recovery due to its magnetic properties.

Materials and Methods Chemicals and materials

Ferric chloride hexahydrate, ferrous sulfate, and zirconium (IV) oxynitrate hydrate were obtained from Sigma-Aldrich (USA). Methanol (99% purity) and ethanol (95% purity), along with diethyl ether, hydrochloric acid, potassium hydroxide, sodium hydroxide, and phenolphthalein, were purchased from Merck Chemicals Co. (Malaysia). These high-quality chemicals were essential for achieving reliable and reproducible results in experimental procedures.

Preparation of Feedstock

The WCO was collected from the Universiti Sains Islam Malaysia cafeteria, where it was used for frying. The WCO was washed with hot water and filtered to eliminate culinary salt and insoluble substances. The oil was then desiccated in an oven heated at 110 °C for 24 h. The acid and saponification properties of the WCO were determined experimentally using standard test methods.

Determination of acid value of feedstock

The acid value of WCO was determined following EN1404 standard method [12]. The acid value test is a critical analysis in biodiesel production, as it provides important information about the free fatty acid (FFA) content in the feedstock (WCO). High FFA content can significantly impact the transesterification process and the efficiency of biodiesel production. In this procedure, 10 g of WCO was precisely weighed into a 250 ml conical flask. The flask was filled with 50 ml of a solvent mixture of 1:1 ethanol and diethyl ether and swiftly shaken to dissolve the oil sample. A few droplets of a 1% phenolphthalein indicator were added to the flask mixture, which was then titrated with vigorous stirring for 10s against a 0.1N standard aqueous solution of KOH until a distinct pink colour persists. The acid value (mg KOH per gram of sample oil) was calculated using the following formula:

Acid value
$$\left(\frac{mg\ KOH}{g\ of\ oil}\right) = \frac{A \times N \times 56.1}{W}$$
 (1)

Where is 56.1 is the KOH's molecular weight (g/mol), KOH normality (mEq/ml), A is the volume of KOH used in titration (ml) and W is the weight of the oil sample (g).

Determination of saponification value of feedstock

Saponification value (SV) is defined as the amount of alkali (expressed in milligrams of potassium hydroxide per gram of sample) required to saponify a specified quantity of sample. It is traditionally determined through saponification of an established amount of fat or oil with excessive KOH solution, subsequently followed by a back titration of the excess base with an acid solution in with the addition of an indicator containing phenolphthalein. The unreacted excess base determines inferentially the base required for the saponification of fatty acyl chains [13]. According to Jain et al. [14], saponification involves oil breakdown with alkali into glycerol and fatty acids. SV is important to test feedstock because it provides crucial information about the feedstock's chemical composition, particularly the average molecular weight of the fats and oils. This process is illustrated in Scheme 1.

Scheme 1. Saponification reaction equation [14]

SV was identified via the AOCS Cd 3a-94 method. In this procedure, 2 g of WCO was properly weighed into a 250 ml conical flask. Approximately 25 mL of ethanolic KOH (0.5N) solution was added while stirring. The flask was then filled with 4 ml of a 1:1 solvent mixture of dehydrated ethanol and diethyl ether and gently shaken to dissolve the oil sample in the solvent mixture. The oil was saponified after being gently heated for 1 h before being cooled to room temperature. Before titration against standardized (0.5N) HCl, a few droplets of phenolphthalein indicator (1%) were added to the sample with vigorous stirring for at least 30 seconds. A second test was performed under the same conditions but without the oil sample. The following formula was used to compute the SV:

Saponification value
$$\left(\frac{mg\ KOH}{g\ of\ oil}\right) = \frac{(B-S)\times N\times 56.1}{W}$$
 (2)

Where B is the titrant volume for blank sample (oil-free mixture) in ml, S is the titrant volume for sample (ml), HCl normality (N), 56.1 is the KOH's molecular weight (g/mol) and W is the weight of the oil sample.

Determination of average molecular weight of feedstock

By applying the following formula, the average molecular weight of WCO was projected from the saponification value [15]:

Average molecular weight =
$$56.1 \times 1000 \frac{3}{SV - AV}$$
 (3)

where SV is the saponification value (AOCS method Cd 3a-94), and AV is the acid value (European Standard EN1404)

Synthesis of Fe₃O₄-ZrO₂ heterogeneous catalyst

The co-precipitation method was used to synthesize ferric oxide nanoparticles. A solution was prepared by combining 60 ml of deionized water with 0.02 M FeSO₄·7H₂O and 0.01 M FeCl₃·6H₂O to maintain a 2:1 molar ratio [16]. The solution was sonicated at 65 °C for 30 min. Separately, 4 M NaOH was prepared in 100 ml of deionized water and added dropwise to the ferric solution until the pH reached 13, resulting in the formation of a black precipitate. The flask was sealed, permitting the reaction to run in the sonicator at a temperature of 65 °C for 1 h. The mixture was permitted to cool at room temperature for 8 min before being centrifuged at 10000 rpm for 8 min. The supernatant was removed, but the black precipitate was kept.

The precipitation was then desiccated in an oven at 40 °C for 24 h [16]. The Fe₃O₄-ZrO₂ catalysts were then synthesized using a straightforward incipient wetness impregnation method. A calculated amount of ferric oxide, corresponding to 10, 20, and 30 wt.% of Fe₃O₄, was dissolved in deionized water, and the required quantity of ZrO₂ was added slowly. At the same time, the solution was stirred at 100 rpm for 5 h. The catalyst was then dried in an oven at 110 °C for 5 h before being calcined at 700 °C. All the synthesized catalysts were subsequently characterized for their physicochemical properties.

Thermogravimetry analysis

Thermogravimetry Analysis (TGA) was performed on a Mettler Toledo instrument from room temperature to 1000 °C at a heating rate of 10 °C min⁻¹ and a N₂ gas flow rate of 20 mL min⁻¹. TGA analysis was utilized to determine the catalysts' thermal stability and degradation actions.

Fourier transform infrared analysis

Fourier Transform Infrared Analysis (FT-IR, Nicolet-iS50) was used to generate an infrared absorption spectrum to identify the functional group and chemical bonds within a molecule, with

scanning performed over a wavenumber range of $400 \text{ to } 4000 \text{ cm}^{-1}$.

Brunauer-Emmett-Teller analysis

Brunauer-Emmett-Teller (BET, analysis Micromeritic) was used to determine the surface area and porosity of the synthesized Fe₃O₄-ZrO₂ catalysts. According to Elumalai Nandhakumar et al. [17], the nitrogen (N2) adsorption and desorption isotherm was obtained by this analysis. The isotherm illustrates the relationship between the quantity of gas adsorbed and the relative pressure. The BET model implies multilayer adsorption and follows a mathematical equation derived from physical assumptions. The BET equation describes the relationship between relative pressure and adsorbate quantity. Analyzing the BET isotherm data and employing the BET equation makes it possible to calculate the catalyst specific surface area. The BET equation is as follows:

$$\frac{1}{X[\binom{P_0}{P}-1]} = \frac{1}{X_m C} + \frac{C-1}{X_m C} \binom{P}{P_0}$$
 (4)

Where X is the weight of the nitrogen adsorbed, X_m is the monolayer capacity and C is the BET constant.

Field emission scanning electron microscopy analysis

Field electron scanning electron microscope (FESEM) was used to capture the morphology of the synthesized catalysts. The samples were evenly dispersed on a sticky carbon tape and coated with a thin layer of gold (Au) to avoid particles charging during the analysis.

Screening of the catalyst

Transesterification was performed in a 100 mL

three-neck glass flask with a water-cooling condenser and thermometer as shown in **Figure 1**. All synthesized catalysts were subjected to transesterification under continuous reaction conditions to identify the most active catalyst for this reaction. The reaction parameters were initially set at methanol to lipid molar ratio of 12: 1 and catalysts loading 5 wt.% at 60 °C for 5 h. Upon completion of the reaction, the layer comprising FAME was recovered and washed with warm water and ethanol to remove saponified byproducts. Below is the equation used for calculating the percentage yield of methyl ester:

Biodiesel yield (%) =
$$\frac{\text{weight of biodiesel}}{\text{weight of oil}} \times 100$$
 (5)

Results and Discussion

Characterization of feedstock

Waste cooking oil (WCO) is increasingly recognized as an exceptional raw material for methyl ester production due to its advantageous properties. These include a high diesel index, favorable pour and cloud points, optimal viscosity, robust cetane number, and specific gravity-qualities comparable to those of virgin oils [19]. This makes WCO an economically and environmentally sustainable choice for biodiesel production, as it repurposes waste while delivering fuel properties suitable for practical applications.

In this study, the potential of WCO as a feedstock for methyl ester production was evaluated by analyzing its acid value and saponification value. These parameters are critical in determining the suitability of the oil for transesterification and its expected yield. **Table 1** presents the detailed physicochemical properties of the designated WCO used in this study.

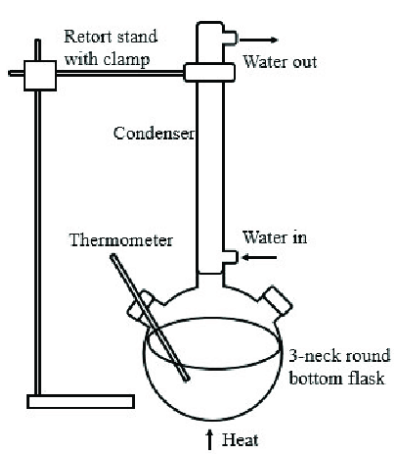


Figure 1. Schematic of the transesterification experimental setup, utilizing an oil bath for temperature control during the reaction [18]

Table 1. The properties of the designated waste cooking oil

| Properties | Unit | Value |
|--------------------------|----------|---------|
| Acid value | mg KOH/g | 1.623 |
| Saponification value | mg KOH/g | 221.018 |
| Average molecular weight | g/mol | 767.110 |

The acid value of the WCO was measured at 1.623 mg KOH/g, indicating the presence of free fatty acids (FFAs) at a concentration of 0.81%. FFAs are chemical compounds generated during the repeated use of cooking oil, often due to hydrolysis and oxidation processes. While a certain level of FFAs is typical for waste cooking oils, a high FFA content exceeding 1% poses challenges for biodiesel production through alkalicatalyzed transesterification. Elevated FFA levels can result in the excessive consumption of the alkali catalyst during the reaction, leading to reduced catalyst performance and significant yield losses [20]. The acid value of WCO prior to transesterification can vary significantly, typically ranging from approximately 1.19 to 10 mg KOH/g, depending on factors such as the type of oil used, duration of use, and storage conditions. For instance, research indicated that WCO with a high acid value of 4.81 mg KOH/g was utilized as feedstock for biodiesel production [21]. These variations highlight the importance of measuring the acid value of WCO before biodiesel production, as higher acid values can impede the transesterification process and may necessitate pre-treatment steps to reduce free fatty acid content.

The saponification value of the waste cooking oil (WCO) was determined to be 221.018 mg KOH/g, which exceeds the value of 198 mg KOH/g reported by Sahar et al. [22]. However, it remains well below the recommended upper limit of 312 mg KOH/g for methyl ester formation. A higher saponification value suggests a higher triglyceride content, which is essential for biodiesel production, while a lower value indicates reduced soap formation an important characteristic for efficient transesterification.

The average molecular weight of the WCO was calculated to be 767.110 g/mol, derived from its acid value and saponification value. This molecular weight is critical for determining the optimal methanol-to-oil molar ratio during the transesterification process. To maximize methyl ester yield, this study employed a methanol-to-oil molar ratio of 12:1, significantly exceeding the stoichiometric requirement. This approach aligns with findings from Suganya et al. [23], who observed that increasing the methanol ratio

reduced both acid value and FFA concentration, improving the efficiency thereby transesterification. Similarly, Munir et al. [24] demonstrated that a 12:1 methanol-to-oil ratio achieved the highest methyl ester yield when using a Cu-Ni/ZrO2 catalyst. This finding is further corroborated by Chingakham et al. [25], who reported that the optimal yield was achieved using a 12:1 molar ratio with CaO as a heterogeneous catalyst. These studies emphasize the importance of excess methanol in enhancing reaction kinetics and overcoming the challenges posed by high FFA content in WCO.

Characterization of catalysts

Four different catalysts were synthesized and utilized in the direct transesterification of waste cooking oil to produce methyl ester. ZrO₂ nanoparticles are interesting due to their increased optical and electrical properties. These allow the nanoparticles to have exceptional mechanical, thermal, and chemical stability, which is beneficial in catalysis field applications [26, 27]. The ZrO₂ catalyst was subsequently impregnated with 10, 20 and 30 wt.% Fe₃O₄, and the resulting magnetized catalysts were designated as 10-Fe-Zr, 20Fe-Zr, and 30Fe-Zr, respectively. The characteristics and catalytic activity of the catalysts were investigated in this study.

Figure 2 presents the TGA curves of uncalcined ZrO₂ and Fe₃O₄. TGA is a crucial method for determining the decomposition temperature and thermal stability of catalysts. The TGA data presented indicates that the Fe₃O₄ and ZrO₂ components of the catalysts exhibit different thermal stability profiles. Below 100°C, the Fe₃O₄-ZrO₂ catalyst experiences weight loss primarily due to the evaporation of physically adsorbed water molecules. This initial weight loss is commonly observed in materials containing hygroscopic components [29]. Above 100 °C, additional weight loss can be attributed to the breakdown of structurally bound water. The significant weight loss observed between 200 °C and 500 °C is likely due to the elimination of residual organic materials and the decomposition of nitrate molecules originating from the synthesis of ZrO₂. This decomposition aligns with the findings [28, 29], who noted similar thermal behavior in iron oxide-based catalysts.

The thermal decomposition processes largely complete around 700 °C, beyond which the weight loss becomes negligible. The TGA results are consistent with those reported by Sapana Guru et al. [30], who observed four distinct stages of mass loss in iron oxide nanoparticles. From their study, the initial mass loss from 50 °C to 300 °C involved the elimination of physically adsorbed H₂O and other guest molecules. The subsequent mass loss from 300 °C to 500 °C was associated with the decomposition of organic materials. The final stages of mass loss, from 500 °C to 750 °C, involved the formation and stabilization of metal oxides. Thus, a calcination temperature of 700 °C is deemed adequate for eliminating organic residues and forming a solid Fe₃O₄-ZrO₂ catalyst with high purity. This temperature facilitates the transesterification process by providing a stable and active catalytic surface. Therefore, all catalysts were calcined in a muffle furnace at 700 °C for 5 hours for further investigation.

FT-IR was used to determine the presence of functional groups in heterogeneous catalyst compounds. Figure 3 shows the FT-IR curves of 10Fe-Zr, 20Fe-Zr and 30Fe-Zr catalysts, along their precursors, FeCl₃.6H₂O FeSO₄.7H₂O. Based on the FT-IR analysis, two wide peaks were observed at 3298.77 cm⁻¹ and 1068.05 cm⁻¹ for FeSO₄.7H₂O precursors, indicating the presence of sulphate groups in the sample. The same findings were observed by Ali et al. [31]. Three distinct peaks were observed at ~3249.77 cm⁻¹, 1595.18 cm⁻¹, and 844.28 cm⁻¹, which can be ascribed to the peaks for FeCl₃.6H₂O precursor [32]. The sulphate and chloride peaks are not observed in the FT-IR spectra of 10Fe-Zr, 20 Fe-Zr and 30Fe-Zr catalysts after calcination at 700 °C.

The FT-IR spectra of Fe₃O₄ displayed strong peaks ranging from 514.25 cm⁻¹ to 685.60 cm⁻¹. These peaks are caused by the stretching vibration mode of the Fe-O bonds within the crystal structure of Fe₃O₄. Furthermore, the Zr-O stretching vibrations were attributed to the distinct absorption peak observed at frequencies below 500 cm⁻¹. This suggests that the synthesized Fe-Zr catalysts were composed solely of metal oxides, with no presence of additional materials. The Fe-Zr catalyst employed is also impervious to the occurrence of undesired reactions that could impede the direct transesterification process to produce methyl ester.

The BET analysis was done to ascertain the surface area and porosity of the synthesized catalysts. The adsorption and desorption of nitrogen were determined through the BET analysis. Figure 4 displays the BET analysis results for Fe₃O₄-ZrO₂ catalysts. As per the classification by the International Union of Pure and Applied Chemistry (IUPAC), all the synthesized ZrO₂ showed a Type IV(a) isotherm because of the creation of adsorption hysteresis [33]. In a separate research, Wang et al. [34] achieved a Type V isotherm for ZrO₂ that was synthesized using the DTAB assisted hydrothermal method and then calcined at 650 °C. This isotherm suggests the disintegration of the highly organized mesoporous structure of ZrO₂. They proposed that when the calcination temperature is high, the size of the crystallite in the sample increases significantly, leading to the collapse of the well-structured mesostructure. The hysteresis loop commonly observed in capillary condensation is attributed to the highly developed mesoporous structures of ZrO₂. Furthermore, specific pore structures have frequently been associated with the shapes of hysteresis loops.

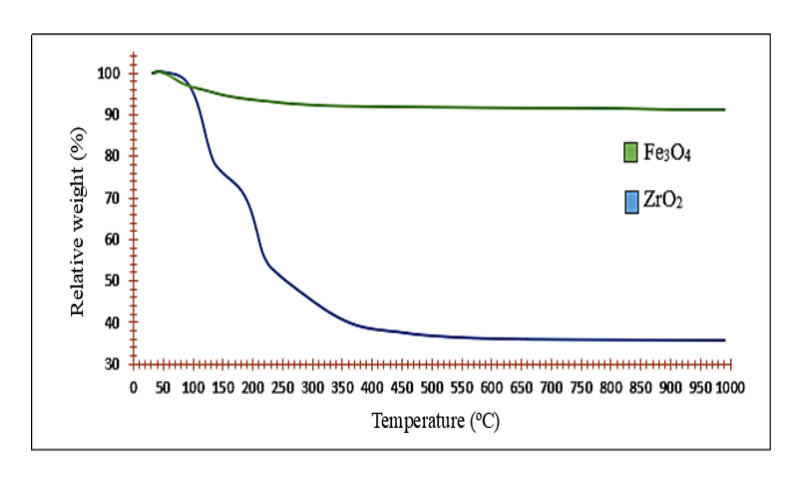


Figure 2. TGA curves of the uncalcined Fe₃O₄ and ZrO₂ catalysts

Malays. J. Anal. Sci. Volume 29 Number 2 (2025): 1311

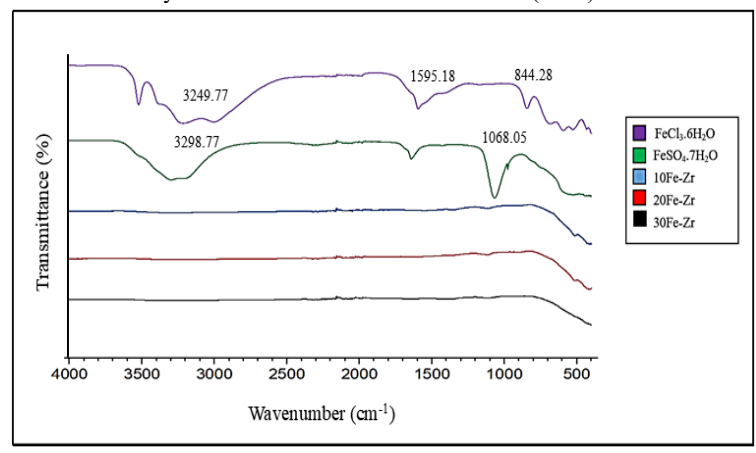


Figure 3. FT-IR curves of the precursors and synthesized catalysts

According to the results in Figure 4, 10Fe-Zr and 20Fe-Zr catalysts resemble hysteresis loop of Type H3 implying loose assemblages of plate-like particles forming slit-like pores. Basahel et al. [33] reported that the lower threshold of the desorption branch is typically found at the cavitation-induced p/p₀. These loops occur when there are non-rigid collections of plate-like particles (such as certain clay) or when the pore network contains macropores that are not entirely filled with pore condensate. Conversely, the 30Fe-Zr catalyst exhibited a Type H1 hysteresis loop. The Type H1 hysteresis loop is typically observed in materials with a limited range of uniform mesopores, where the width of the neck size distribution is comparable to the width of the pore size [35].

Table 2 shows the surface area, pore volume and average pore size of all the synthesized catalysts. Based on the results, the surface area of the catalyst shows a decreasing trend by increasing the proportion of metal oxide in the catalyst. As the concentration of metals impregnated in the catalyst increased, metal accumulation in the pores or uneven distribution on the surface of the catalyst occurred, leading to a decrease in nitrogen adsorption on the specific surface area. 20Fe-Zr catalyst shows the highest amount of pore volume which is 0.282 cm³/g with relatively high average pore size (5.560 nm) compared to the other synthesized catalysts. Based on the pore size, all the synthesized catalysts exhibit a mesoporous structure, ranging between 2 to 50 nm.

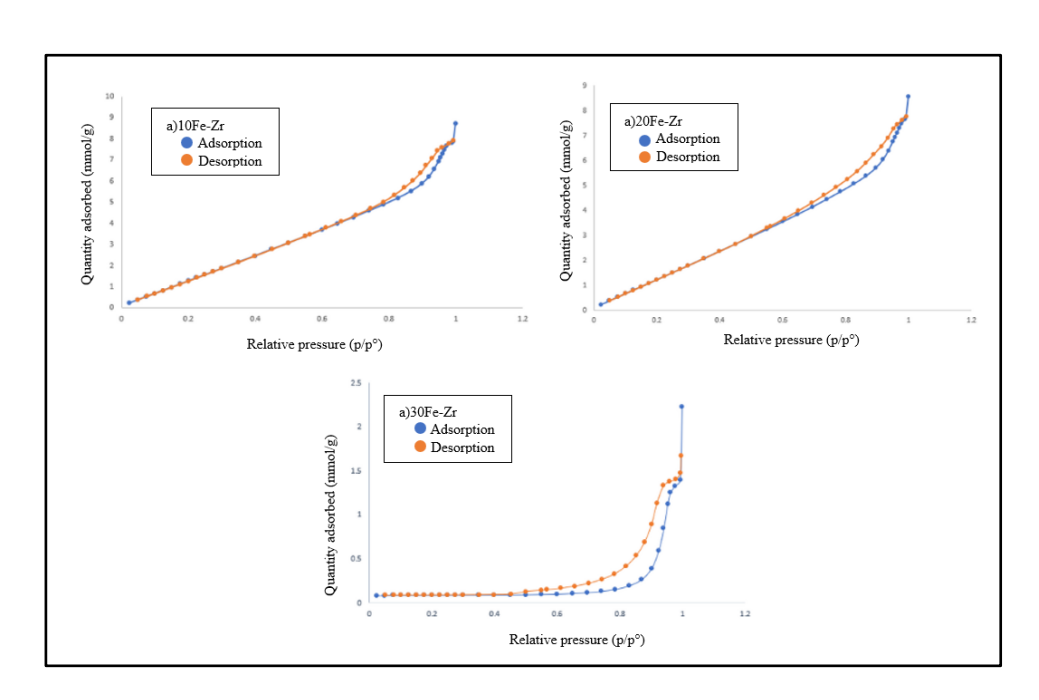


Figure 4. N₂ adsorption-desorption isotherms of 10Fe-Zr, 20Fe-Zr and 30Fe-Zr catalysts

Table 2. Textural properties of 10Fe-Zr, 20Fe-Zr and 30Fe-Zr catalysts

| Catalyst | Surface Area (m²/g) | Pore Volume (cm ³ /g) | Average Pore Size (nm) |
|----------|------------------------|-------------------------------------|------------------------|
| 10Fe-Zr | 206.0426 | 0.270309 | 5.2476 |
| 20Fe-Zr | 203.1300 | 0.282361 | 5.5602 |
| 30Fe-Zr | 189.6763 | 0.276308 | 5.8269 |

The morphology of the synthesized catalysts was analyzed using FESEM. The advanced imaging capabilities of **FESEM** facilitated comprehensive analysis of the catalysts' porosity and surface morphology. Figures 5 a-e display the FESEM images of the catalyst, illustrating its porous nature that facilitates the catalytic reaction sites. From the FESEM images, it can be seen that pure ZrO₂ exhibits rougher surface as compared to pure Fe₃O₄ with non-obvious grain boundary. On the other hand, pure Fe₃O₄ shows a mixture of small and agglomeration of particles. Increasing the Fe₃O₄ loading from 10 to 30 wt.% resulted in the formation of agglomerates due to the dispersion of Fe₃O₄ particles on the ZrO₂ surface. This phenomenon contributed to a reduction in the surface area of the catalysts with higher Fe₃O₄ dopant loadings, as confirmed by BET analysis. Similar findings were reported by Rahman et al. [36] during the synthesis of Bi₂O₃/ZrO₂ catalysts for biodiesel production from microalgae oil.

Screening of catalytic performance

The synthesized catalysts were then employed in the direct transesterification of WCO to produce methyl ester. **Figure 6** compares the catalytic performance of Fe-Zr catalysts and single ZrO₂ at fixed reaction conditions, i.e., methanol to WCO molar ratio of 12:1, 5 wt.% catalyst loading, 60 °C reaction temperature, and continuous stirring at 350 rpm for 3 hours. The results indicate that 20Fe-Zr possesses the highest methyl ester yield followed by ZrO₂, 10Fe-Zr, and 30Fe-Zr catalysts. Additionally, the acid value of the synthesized biodiesel was calculated to be 0.435 mg KOH/g, indicating the successful conversion process and the reduction of free fatty acids. A high acid value is often indicative of severe oil oxidation or the depletion of lubricating properties, which can increase the risk of internal corrosion in engines when the biodiesel is utilized. According to Sahar et al. [22], the acid value for the methyl should be less than 0.8 mg KOH/g. Zhang et al. [37] discovered that the catalytic efficiency of catalysts is attributed to the presence of active sites located within the different oxides. In another study, Guldhe et al. [38] reported a high methyl ester yield from WCO using WO₃/ZrO₂ as a catalyst. Similarly, Booramurthy et al. [39] successfully converted WCO to over 90% methyl ester using an Fe-MnSO₄/ZrO₂ catalyst under optimal reaction conditions of 65°C and a reaction time of 5 hours.

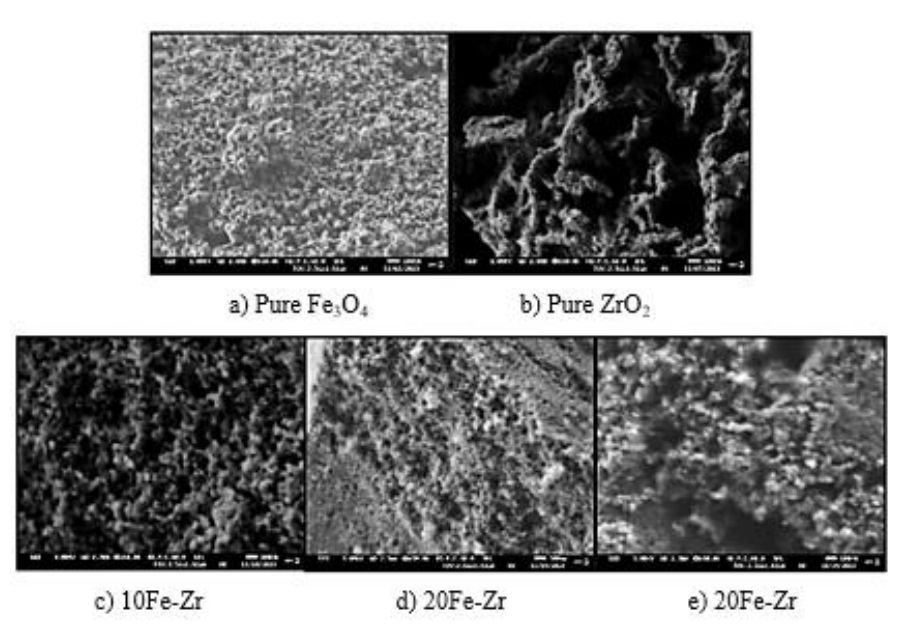


Figure 5 a-e. FESEM images of the catalyst at 50KX magnifications

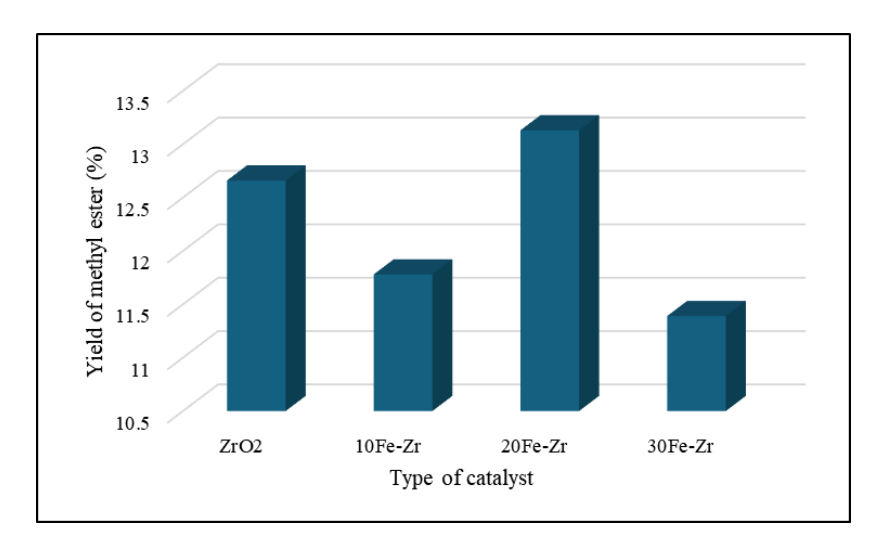


Figure 6. Methyl ester yields using different catalysts

In the following experiment, the 20Fe-Zr catalyst was chosen as the most effective catalyst for the synthesis of methyl ester from WCO. Despite the methyl ester yields not attaining greater than 90%, in this preliminary study, the synthesized catalysts possess magnetic characteristics that facilitate its easy retrieval using a magnet once the process is finished. Further optimization study should be conducted in future involving different factors such as stirring rate, oil to methanol ratio, catalyst dosage, and different reaction temperatures, to maximize the methyl ester yield. Understanding the acidic and basic properties of catalysts allows for selecting or designing the most suitable catalyst for a given feedstock and reaction conditions. This ensures high biodiesel yield, minimizes by-products, and improves overall process efficiency. In addition, advanced analytical techniques should be employed such as GC or high-performance liquid chromatography (HPLC), to quantify ester content and confirm biodiesel purity more accurately. This will provide a more comprehensive understanding of the catalyst's performance, and the quality of the biodiesel produced.

The synthesized catalysts were utilized for the direct transesterification of WCO to produce methyl esters. Figure 6 compares the catalytic performance of Fe-Zr catalysts with single ZrO₂ under fixed reaction conditions: a methanol to WCO molar ratio of 12:1, 5 wt.% catalyst loading, reaction temperature of 60°C, and continuous stirring at 350 rpm for 3 hours. Among the tested catalysts, 20Fe-Zr exhibited the highest methyl ester yield, followed by ZrO₂, 10Fe-Zr, and 30Fe-Zr. The enhanced catalytic activity of the 20Fe-Zr catalyst is attributed to its mesopore connectivity,

high pore volume, and large surface area. Additionally, the acid value of the synthesized biodiesel was measured at 0.435 mg KOH/g, signifying a successful conversion process and a significant reduction in FFAs. A high acid value can indicate severe oil oxidation or degraded lubricating properties, which may lead to internal engine corrosion when biodiesel is utilized. According to Sahar et al. [22], the acid value for methyl esters should be below 0.8 mg KOH/g to meet biodiesel quality standards. The catalytic efficiency observed in this study aligns with findings by Zhang et al. [37], who attributed catalytic activity to the presence of active sites within various oxides. Guldhe et al. [38] reported a high methyl ester yield from WCO using WO₃/ZrO₂ as a catalyst. Similarly, Booramurthy et al. [39] achieved over 90% methyl ester conversion using Fe-MnSO₄/ZrO₂ under optimal conditions of 65°C and a reaction time of 5 hours. In the current study, the 20Fe-Zr catalyst was identified as the most effective for synthesizing methyl esters from WCO.

While the yields in this preliminary investigation did not exceed 90%, the synthesized catalysts exhibited magnetic properties, enabling easy recovery using a magnet after the reaction. Future studies should focus on optimizing reaction parameters, including stirring rate, methanol-to-oil ratio, catalyst dosage, and reaction temperature, to maximize methyl ester yield. Furthermore, understanding the acidic and basic properties of the catalysts is crucial for selecting or designing the most suitable catalyst for specific feedstocks. Advanced analytical techniques such as gas chromatography (GC) or high-performance liquid chromatography (HPLC) should also be employed

to accurately quantify ester content and confirm biodiesel purity. These approaches will provide a more comprehensive understanding of the catalyst's performance, and the quality of the biodiesel produced.

Conclusion

study successfully synthesized This characterized magnetized Fe₃O₄-ZrO₂ catalysts for the direct transesterification of waste cooking oil to biodiesel. Among the synthesized catalysts, superior 20Fe-Zr demonstrated performance, achieving a methyl ester yield of 13.13%. This enhanced activity is attributed to its mesoporous structure, high pore volume, and large surface area, which facilitate effective reactant diffusion and catalytic interactions. incorporation of magnetic Fe₃O₄ further enables easy separation and recovery of the catalyst, enhancing reusability and reducing process costs. The results highlight the potential of magnetized Fe₃O₄-ZrO₂ catalysts as efficient and sustainable alternatives for biodiesel production. However, the relatively moderate yield observed suggests the need for further optimization of reaction parameters to maximize efficiency.

Acknowledgement

This research was funded by Universiti Sains Islam Malaysia under the Research Grant USIM (PPPI/TAMHIDI/0122/USIM/16222).

References

- 1. Shay, E.G. (1993). Diesel fuel from vegetable oils: Status and opportunities. *Biomass Bioenergy*, 4(4): 227-242.
- 2. Ma, F., and Hanna, M.A. (1999). Biodiesel production: A review. *Bioresource Technology*, 70(1): 1-15.
- 3. Belousov, A.S., Esipovich, A.L., Kanakov, E.A., and Otopkova, K.V. (2021). Recent advances in sustainable production and catalytic transformations of fatty acid methyl esters. *Sust. Energy Fuels*, 5(18): 4512-4545.
- Miyuranga, K.A.V., Arachchige, U.S.P.R., Marso, T.M.M., and Samarakoon, G. (2023). Biodiesel production through the transesterification of waste cooking oil over typical heterogeneous base or acid catalysts. Catalysts, 13(3): 546.
- 5. Nigatu G.S., and Mario M.J. (2017). Biodiesel production technologies: review. *AIMS Energy*, 5(3): 425-457.
- Su, G., Hwai C.O., Ibrahim, S., Fattah, R., Mofijur, M. and Cheng T. C. (2021). Valorisation of medical waste through pyrolysis for a cleaner environment: Progress and challenges. *Environmental Pollution*, 279: 116934.

- Hazrat, M.A., Rasul, M.G., Mohammad, N.A., Silitonga, A.S., Fattah, R., and Indra, M. (2022). Kinetic modelling of esterification and transesterification processes for biodiesel production utilising waste-based resource. Catalysts, 12(11): 1472.
- 8. Ma'arof, N.A.N.B., Hindryawati, N., Khazaai, S.N.M., Bhuyar, P., Rahim, M.H.A., and Maniam, G.P. (2021). Biodiesel (methyl esters). *Maejo International Journal of Energy and Environmental Communication*, 3(1): 30-43.
- Nayab, R., Imran, M., Ramzan, M., Tariq, M., Taj, M.B., Akhtar, M. N., and Iqbal, H.M. (2022). Sustainable biodiesel production via catalytic and non-catalytic transesterification of feedstock materials—A review. *Fuel*, 328: 125254.
- Santoso, A., None Sumari, Salim, A., and Siti Marfu'ah. (2018). Synthesis of methyl ester from chicken oil and methanol using heterogeneous catalyst of CaO-MgO as well as characterization its potential as a biodiesel fuel. *Journal Physics Conference Series*, 1093: 012035.
- 11. Thanh, L. T., Okitsu, K., Boi, L. V., and Maeda, Y. (2012). Catalytic technologies for biodiesel fuel production and utilization of glycerol: a review. *Catalysts*, 2(1): 191-222.
- Santos, E. P., De Souza, E. F., Ramos, T. C., Da Silva, M. S., and Fiorucci, A. R. (2018). Evaluation of potentiometric methods for acid number determination in commercial biodiesel samples and proposal of alternative method. *Orbital: Electronic Journal Chemistry*, 10(1): 47-53.
- 13. Ivanova, M., Hanganu, A., Dumitriu, R., Tociu, M., Ivanov, G., Stavarache, C., Popescu, L., Ghendov-Mosanu, A., Sturza, R., Deleanu, C., and Chira, N.-A. (2022). Saponification value of fats and oils as determined from ¹H-NMR data: The case of dairy fats. *Foods*, 11(10): 1466.
- 14. Jain, B.P., Goswami, S.K., Pandey, S., Jain, B.P., Goswami, S.K., and Pandey, S. (2021). Chapter 3 Lipid. In *Protocol Biochemistry Clininical Biochemistry*, 23-30.
- 15. Anastopoulos, G., Zannikou, Y., Stournas, S., and Kalligeros, S. (2009). Transesterification of vegetable oils with ethanol and characterization of the key fuel properties of ethyl esters. *Energies*, 2(2): 362-376.
- 16. Yadav, V.K., Ali, D., Khan, S. H., Gnanamoorthy, G., Choudhary, N., Yadav, K.K., Thai, V.N., Hussain, S. A., and Manhrdas, S. (2020). Synthesis and characterization of amorphous iron oxide nanoparticles by the sonochemical method and their application for the remediation of

- heavy metals from wastewater. *Nanomaterials*, 10(8): 1551.
- Nandhakumar, E., Priya, P., Rajeswari, R., Aravindhan, V., Sasikumar, A., and Senthilkumar, N. (2019). Studies on structural, optical and thermal properties of Fe₃O₄ (NR)/ZrO₂ CSNCs synthesized via green approach for photodegradation of dyes. Research on Chemical Intermediates, 45: 2657-2671.
- 18. Ahmad, M. A., & Samsuri, S. (2021). Biodiesel purification via ultrasonic-assisted solvent-aided crystallization. *Crystals*, 11(2): 212.
- 19. Owolabi R.U., Osiyemi N.A., Amosa M.K., and Ojewumi M.E. (2011). Biodiesel from household/restaurant waste cooking oil (WCO). *Journal Chemical Engineering Processing Technology*, 2(4): 1000112.
- 20. Yusuff, A. S., Adeniyi, O. D., Olutoye, M. A., and Akpan, U. G. (2019). Waste frying oil as a feedstock for biodiesel. *Petroleum Chemicals: Recent Insight*, 2: 5-29.
- 21. Hsiao, M. -C., Liao, P. -H., Lan, N. V., and Hou, S. -S. (2021). Enhancement of biodiesel production from high-acid-value waste cooking oil via a microwave reactor using a homogeneous alkaline catalyst. *Energies*, 14(2): 437.
- Sadaf, S., Iqbal, J., Ullah, I., Bhatti, H. N., Nouren, S., Nisar, J., and Iqbal, M. (2018). Biodiesel production from waste cooking oil: an efficient technique to convert waste into biodiesel. Sustainable Cities and Society, 41: 220-226.
- Suganya, T., Gandhi, N. N., and Renganathan, S. (2013). Production of algal biodiesel from marine macroalgae *Enteromorpha compressa* by two step process: optimization and kinetic study. *Bioresource Technology*, 128: 392-400.
- 24. Munir, M., Ahmad, M., Saeed, M., Waseem, A., Nizami, A. S., Sultana, S., ... and Ali, M. I. (2021). Biodiesel production from novel non-edible caper (*Capparis spinosa* L.) seeds oil employing Cu–Ni doped ZrO₂ catalyst. *Renewable and Sustainable Energy Reviews*, 138: 110558.
- 25. Chingakham, C., Tiwary, C., and Sajith, V. (2019). Waste animal bone as a novel layered heterogeneous catalyst for the transesterification of biodiesel. *Catalysis Letters*, 149: 1100-1110.
- Rahulan, K. M., Vinitha, G., Stephen, L. D., and Kanakam, C. C. (2013). Synthesis and optical limiting effects in ZrO₂ and ZrO₂@ SiO₂ core—shell nanostructures. *Ceramics International*, 39(5): 5281-5286.
- 27. Banić, N., Šojić Merkulov, D., Despotović, V., Finčur, N., Ivetić, T., Bognár, S., Jovanović,

- D., and Abramović, B. (2022). Rapid removal of organic pollutants from aqueous systems under solar irradiation using ZrO₂/Fe₃O₄ nanoparticles. *Molecules*, 27(22): 8060.
- Mishra, V.K., and Goswami, R. (2017). A review of production, properties and advantages of biodiesel. *Biofuels*, 9(2): 273-289
- Kristianto, Y., Taufik, A., and Saleh, R. (2017).
 Photo-, sono-and sonophotocatalytic degradation of methylene blue using Fe₃O₄/ZrO₂ composites catalysts. *AIP Conference Proceedings*, 1862: 030017.
- 30. Guru, S., Mishra, D., Amritphale, S. S., and Joshi, S. (2016). Influence of glycols in microwave assisted synthesis of ironoxide nanoparticles. *Colloid and Polymer Science*, 294: 207-213.
- 31. Ali, Q., Ali, S., El-Esawi, M. A., Rizwan, M., Azeem, M., Hussain, A. I., ... and Wijaya, L. (2020). Foliar spray of Fe-Asp confers better drought tolerance in sunflower as compared with FeSO₄: Yield traits, osmotic adjustment, and antioxidative defense mechanism. *Biomolecules*, 10(9): 1217.
- 32. Muhammad Inam, Khan, R., Park, D., Lee, Y.-W., and Yeom, I. (2018). Removal of Sb(III) and Sb(V) by ferric chloride coagulation: Implications of Fe solubility. *Water*, 10(4): 418-418.
- 33. Basahel, S.N., Mokhtar, M., Edreese Alsharaeh, Ali, T.T., Mahmoud, H.A., and Katabathini, N. (2016). Physico-chemical and catalytic properties of mesoporous CuO-ZrO₂ Catalysts. *Catalysts*, 6(4): 57-57.
- 34. Wang, H., Covarrubias, J., Prock, H., Wu, X., Wang, D., and Bossmann, S.H. (2015). Acid-functionalized magnetic nanoparticle as heterogeneous catalysts for biodiesel synthesis. *Journal Physics Chemistry C*, 119(46): 26020-26028.
- 35. Yang, L., Wu, H., Jia, J., Ma, B., and Li, J. (2017). Synthesis of bimodal mesoporous silica with coexisting phases by cohydrothermal aging route with P123 containing gel and F127 containing gel. *Microporous Mesoporous Materials*, 253: 151-159.
- 36. Rahman, N.J.A., Ramli, A., Jumbri, K., and Uemura, Y. (2019). Tailoring the surface area and the acid-base properties of ZrO₂ for biodiesel production from Nannochloropsis sp. *Scientific Report*, 9(1): 16223.
- 37. Zhang, Z., Han, D., Wei, S., and Zhang, Y. (2010). Determination of active site densities and mechanisms for soot combustion with O₂ on Fe-doped CeO₂ mixed oxides. *Journal Catalyst*, 276(1): 16-23.

- 38. Guldhe, A., Singh, P., Ansari, F. A., Singh, B., and Bux, F. (2017). Biodiesel synthesis from microalgal lipids using tungstated zirconia as a heterogeneous acid catalyst and its comparison with homogeneous acid and enzyme catalysts. *Fuel*, 187: 180-188.
- 39. Booramurthy, V. K., Kasimani, R., Pandian, S., and Ragunathan, B. (2020). Nano-sulfated zirconia catalyzed biodiesel production from tannery waste sheep fat. *Environmental Sciences Pollution Research*, 27(17): 20598-20605.